11-2015

Tungsten Disulphide Based All Fiber Q-Switching Cylindrical-Vector Beam Generation

J. Lin
University of Science and Technology of China

K. Yan
University of Science and Technology of China

Yong Zhou
University of Science and Technology of China

L. X. Xu
University of Science and Technology of China

C. Gu
University of Science and Technology of China

See next page for additional authors

Tungsten disulphide based all fiber Q-switching cylindrical-vector beam generation

J. Lin,[1] K. Yan,[1] Y. Zhou,[1] L. X. Xu,[1,2,a)] C. Gu,[1,2] and Q. W. Zhan[3]
[1]*Department of Optics and Optical Engineering, University of Science and Technology of China, Hefei 230026, China*
[2]*Haixi Collaborative Innovation Center for New Display Devices and Systems Integration, Fuzhou University, Fuzhou 350002, China*
[3]*Electro-Optics Program, University of Dayton, Dayton, Ohio 45469, USA*

(Received 6 August 2015; accepted 29 October 2015; published online 12 November 2015)

We proposed and demonstrated an all fiber passively Q-switching laser to generate cylindrical-vector beam, a two dimensional material, tungsten disulphide (WS_2), was adopted as a saturable absorber inside the laser cavity, while a few-mode fiber Bragg grating was used as a transverse mode-selective output coupler. The repetition rate of the Q-switching output pulses can be varied from 80 kHz to 120 kHz with a shortest duration of 958 ns. Attributed to the high damage threshold and polarization insensitivity of the WS_2 based saturable absorber, the radially polarized beam and azimuthally polarized beam can be easily generated in the Q-switching fiber laser. © *2015 AIP Publishing LLC*. [http://dx.doi.org/10.1063/1.4935465]

Since the first successful fabrication of graphene, two dimensional (2D) materials have attracted growing attention attributed to their various applications in photonic and optoelectronic devices.[1–3] One of the important applications of the 2D materials is the saturable absorber (SA), which has been widely used to generate mode-locked or Q-switching laser pulses. Since the demonstration of graphene based mode-locked fiber laser,[4,5] many setups were presented.[6,7] After that, topological insulator (TI), a new 2D material with a new state of quantum matter with the metallic states on the surface, was first proved having the saturable absorption effect in the third telecommunication window,[8] and TI-based passively mode-locked and Q-switching fiber lasers have been experimentally realized.[9–11] Recently, molybdenum disulfide (MoS_2), one of a 2D semiconducting transition metal dichalcogenides (TMDs), despite the wide direct and indirect bandgap, has been demonstrated the saturable absorption effect in a wide band by deliberately introducing the defects[12] or from the edge-related sub-bandgap states.[13] Both the passively mode-locked and Q-switching lasers based on layered MoS_2[14–16] have been achieved. Another kind of TMDs, tungsten disulphide (WS_2), with ultra-high optical damage threshold,[17] unusually large second order nonlinear susceptibility[18] and large nonlinear refractive index,[19] has also been demonstrated saturable absorption and WS_2-based pulsed lasers have been successfully fabricated,[17,20] indicating the promising prospect for ultrafast photonic applications.

In 2012, Sobon *et al*. successively demonstrated linearly polarized mode-locked and Q-switched erbium doped fiber laser based on graphene or reduced graphene oxide saturable absorber.[21,22] The cavity was designed using only polarization maintaining fibers and components, resulting in linearly polarized output beam with degree of polarization at the level of nearly 100%. Linearly polarized light is one of the spatially homogeneous states of polarization (SOP) and does not depend on the spatial location in the beam cross section. Besides, there is another kind of light beams with spatially variant SOP.[23] Cylindrical vector beam (CVB) is one particular example, which contains radially polarized beam and azimuthally polarized beam. CVB was earliest discovered in experiment by Pohl in 1972,[24] but it caught little attention at first. In recent years, there has been an increasing interest in CVB, for their unique properties under high numerical-aperture (NA) focusing.[25,26] Till date, this laser beam with cylindrical symmetry in polarization leads to a range of applications such as optical tweezers,[27] surface plasmon excitation,[28] high-resolution microscopy,[29] material processing,[30] and optical data transmission.[31] Various kinds of continuous-wave (CW) CVBs have already been demonstrated.[32,33] In order to achieve high energy, some works proposed to generate Q-switching CVBs,[34] but all of them were focused on solid structure and all-fiber configuration has never been reported. The key elements to achieve Q-switching CVBs are a transverse mode selector and a suitable saturable absorber. Among various transverse mode selectors (calcite crystal, sub-wavelength gratings, and spatial light modulator, etc), FM-FBG has been proved to be an efficient method when the laser operates within a narrow spectrum. On the other hand, compared with traditional SAs, the aforementioned WS_2 overcomes the low damage threshold and high expense of semiconductor saturable absorber mirrors (SESAMs) and the sensitivity to polarization and environmental changes of artificial SAs such as nonlinear amplifying-loop mirrors (NALMs) and nonlinear polarization rotation (NPR). The saturable absorption of WS_2 has already been demonstrated at the wavelengths of 532 nm,[35] 800 nm,[19] 1064 nm,[36] 1550 nm,[17,20] and 1940 nm,[37] indicating its ultra-wide operation band. What is more, WS_2 shows high transmittance from visible to infrared as shown below, which can reduce the insertion loss in fiber lasers. So WS_2 is predicted to be an ideal saturable absorber to achieve an all-fiber passively Q-switching CVBs, and this compact and alignment-free configuration will dramatically expand the prospect of applications.

a)Author to whom correspondence should be addressed. Electronic mail: xulixin@ustc.edu.cn.

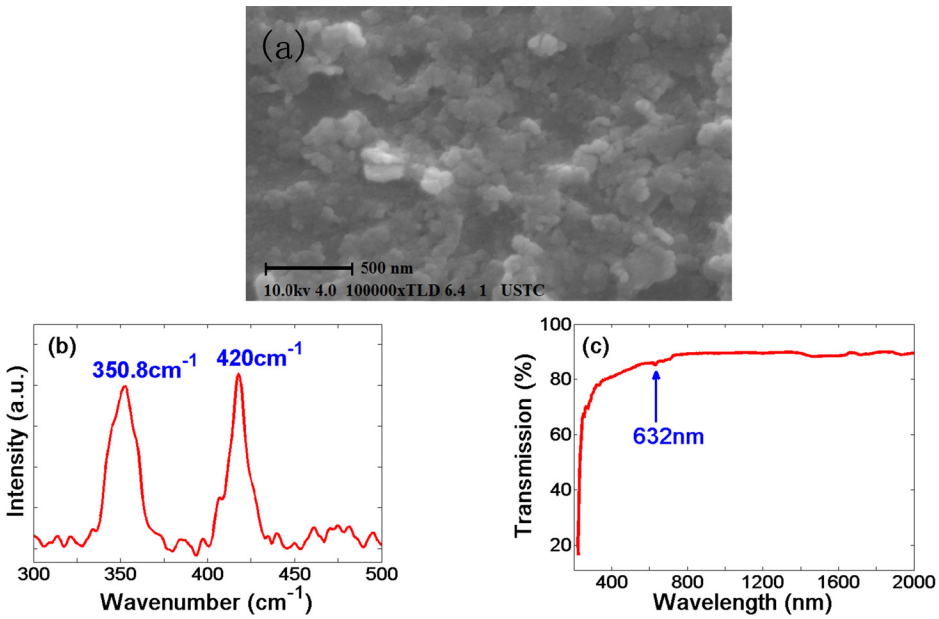

FIG. 1. (a) The SEM image of WS_2 nanoplates. (b) The Raman spectrum of the WS_2-PVA film. (c) The linear transmission spectrum of the WS_2-PVA film.

In this letter, we report an all-fiber laser generating Q-switching CVB by using WS_2 as a SA and a FM-FBG as a transverse mode selector. The repetition rate of the Q-switching pulses can be tuned from 80 kHz to 120 kHz. The minimum pulse duration achieved is 958 ns. Both the high purity radially polarized beam and azimuthally polarized beam in Q-switching state can be obtained just by adjusting the polarization controllers (PCs).

The WS_2 nanoplates used in our experiment were obtained by lithium-based chemical exfoliation[38] and then dispersed in deionized water with a concentration of 0.1 mg/ml. Figure 1(a) shows the scanning electron microscopy (SEM) image of the WS_2 nano-sheets. The flakes diameter falls in the range of 20–500 nm. Then we added 0.4 g polyvinylalcohol (PVA) powder into the WS_2 solution and ultrasonically agitated for ~8 h. The WS_2-PVA solution was dropped on a Petri dish and slow evaporated in an oven at 45 °C, resulting in a PVA-composite film. We characterized the Raman spectrum of the WS_2-PVA using Ar^+ laser at 514 nm, as depicted in Fig. 1(b). The characteristic bands at 350.8 and 420 cm^{-1} on the Raman spectrum can be clearly observed, corresponding to the in-plane (E^1_{2g}) and out-of-plane (A_{1g}) vibrational modes of WS_2.[39] We also measured the linear transmission spectrum of the WS_2-PVA film [Fig. 1(c)]. The dip near 632 nm in the transmission spectrum is a typical fingerprint of WS_2 nanosheets due to the direct bandgap transition.[40] The spectrum beyond 700 nm shows an almost flat curve, indicating its broadband optical response.

The saturable absorption property of the prepared WS_2-PVA thin film has been investigated by open-aperture Z-scan technology with a homemade picosecond fiber laser centered at 1550 nm. The Z-scan curve and corresponding nonlinear saturable absorption curve are shown in Figs. 2(a) and 2(b). Through fitting the curve, the saturable intensity and the modulation depth were measured and calculated of 13 MW/cm^2 and 1.4%. The physical mechanism behind the saturable absorption of the WS_2 is that electrons from the valence band are excited into the conduction band for absorption of light. When under intense illumination, energy levels in the conduction band are filled, and further absorption is blocked due to Pauli blocking.[4] The diameter of the WS_2 flakes used in our experiment falls in the range of 20–500 nm, resulting in a large edge to surface area ratio, so in spite of operating below the material bandgap, the WS_2 still exhibits saturable absorption from the edge-related sub-bandgap states. In order to assemble the WS_2-PVA film into fiber laser, we placed one small piece between two fiber connectors and formed a fiber-compatible SA.

Figure 3 shows the schematic of the passively Q-switching fiber laser to generate CVB based on the WS_2 saturable absorber, which consists of a 974 nm pumping laser diode (LD), a 980 nm/1550 nm wavelength division multiplexer (WDM), a 60 cm highly erbium doped fiber (Liekki Er110-8/125), a 3-ports circulator, two polarization controllers (PC-1 and PC-2), an offset splice spot (OSS), a few mode fiber Bragg grating (FM-FBG), a WS_2-PVA based SA, and an output

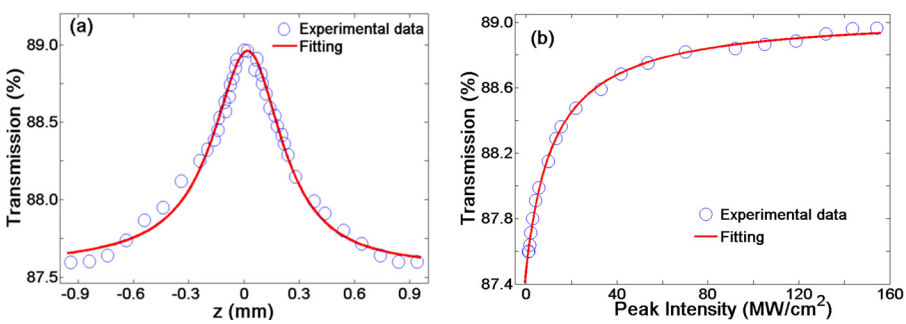

FIG. 2. (a) The Z-scan curve of the WS_2-PVA film at 1550 nm. (b) The corresponding nonlinear saturable absorption curve.

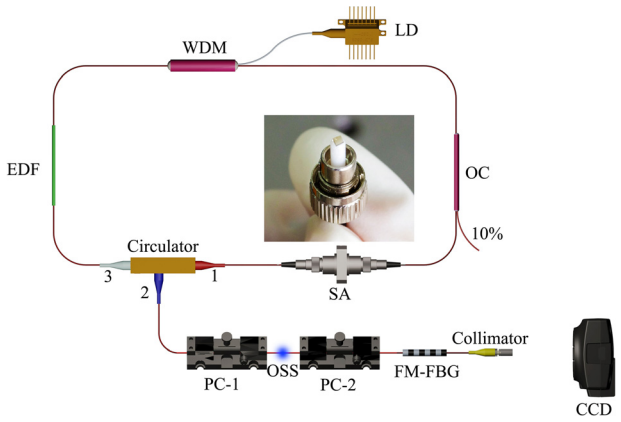

FIG. 3. The experimental setup of the Q-switching fiber laser. Inset: the photograph of the WS_2-PVA film on the fiber connector.

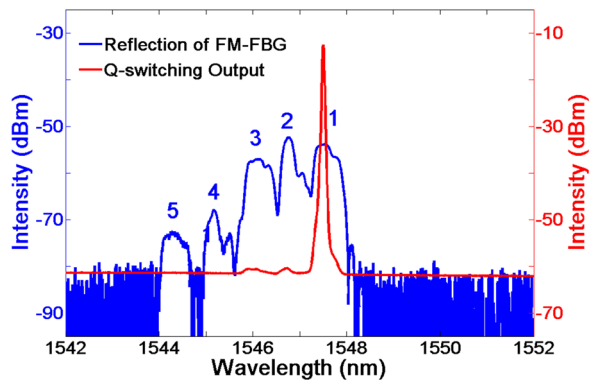

FIG. 4. Reflection spectrum of FM-FBG (blue) and Q-switching output spectrum (red).

coupler (OC). The FM-FBG is used as a transverse mode-selective output coupler, which was fabricated in a few-mode photosensitive fiber with a NA number of 0.12 with core and clad diameter of 19 μm and 125 μm, Thus, the fiber can support four linearly polarized (LP) modes around 1550 nm, including the 1st order mode (LP01), the 2nd order mode (LP11), and the 3rd order mode (LP21 and LP02), respectively. There are five reflection peaks on the spectrum corresponding with five reflections between different order modes, as shown in Fig. 4 with blue curve. Peak 1 represents the 1st to 1st order mode reflection, peak 2 represents the 1st to 2nd order mode reflection, peak 3 represents the 2nd to 2nd order mode reflection, peak 4 represents the 2nd to 3rd order mode reflection, and peak 5 represents the 3rd to 3rd order mode reflection. The FM-FBG is connected by a circulator. Two fiber polarization controllers (PC-1 and PC-2) were placed on each sides of an OSS. The OSS was formed through splicing two section fibers with a 3.1-μm lateral misalignment, which provided stable and efficient coupling from the fundamental mode to high order modes.[41] The WS_2-PVA based SA was placed between the output coupler and the circulator. A 9:1 output coupler was used to output the laser emission through the 10% port. The total length of the cavity was ~7 m. The Q-switching laser output was measured by an optical spectrum analyzer and a 4 GHz digital oscilloscope, the transverse distribution of the intensity was output through a collimator connected to the end of the FM-FBG and recorded by a 1550 nm CCD camera.

When the pump power increased to 290 mW, the stable Q-switching laser pulse appeared. The repetition rate of the Q-switching laser was observed pump-dependent up to our maximum available power of 600 mW, which is the typical feature of Q-switching laser. The temporal behavior of the pulse train and the single pulse shape at a pump power of 315 mW are shown in Figs. 5(a) and 5(b). The repetition rate was 84.12 kHz with the full width at half maximum (FWHM) of 2.26 μs. The Q-switching spectrum is shown in Fig. 4 with red curve. The spectrum centered at 1547.5 nm and the width at 30 dB depth was 0.14 nm. The operating wavelength was within the peak 1 of the reflection spectrum of FM-FBG, which represents the 1st to 1st order mode reflection, so the FM-FBG worked as an efficient fundamental mode reflector

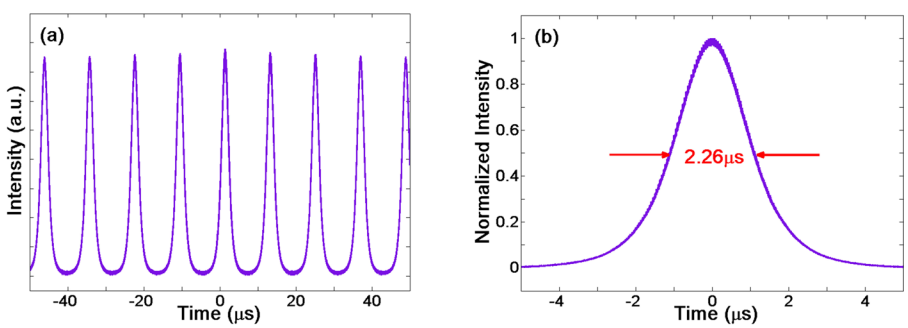

FIG. 5. (a) Typical pulse train for 315 mW pump power. (b) The corresponding single pulse envelope.

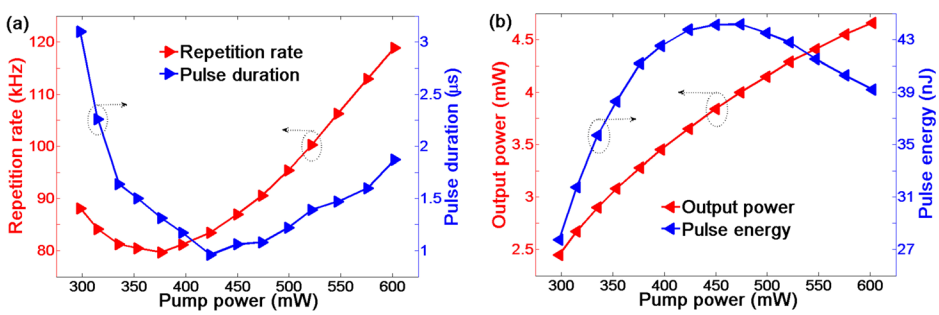

FIG. 6. (a) The pulse repetition rate and duration versus the pump power. (b) The output power and pulse energy versus the pump power.

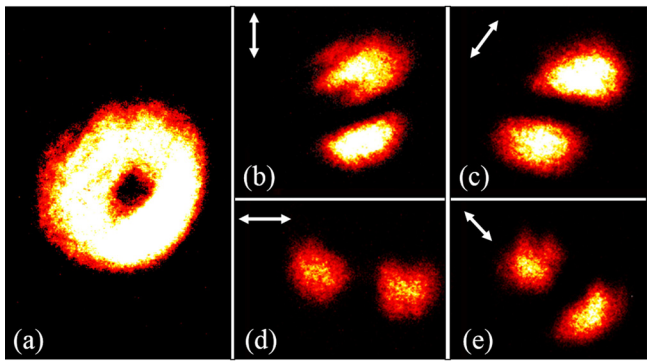

FIG. 7. Intensity distributions of radially polarized laser beam. (a) Radially polarized without a polarizer; (b) and (e) radially polarized after passing through a linear polarizer with transmission axis orientation denoted by arrows.

and only allowed the higher modes passing though. That would greatly increase the mode purity of the output beam.

Fig. 6(a) shows the pulse duration and the pulse repetition rate as a function of the pump power. By increasing the pump power, the repetition rate fell off a little at first and then increased monotonically, similar to reference.17 The repetition rate varied from 80 kHz to 120 kHz, with a range of 40 kHz, when the pump power increased from 290 mW to 600 mW, while the output power increased from 2.44 mW to 4.66 mW [as shown in Fig. 6(b)]. The pulse energy rapidly grew in the initial stage, but after the pump power beyond 450 mW, the pulse energy came to saturate. The maximum pulse energy measured was 44 nJ and the minimum duration achieved was 958 ns.

A high purity radially polarized beam was obtained by carefully tuning PC-1 and PC-2. The doughnut intensity profile of the radially polarized output mode was shown in Fig. 7(a). After passing through a linear polarizer under four different orientations, the intensity distributions are shown in Figs. 7(b)–7(e), respectively, demonstrating the radially polarized output.

A high purity azimuthally polarized beam was also obtained by tuning PC-1 and PC-2. The specific intensity distributions of the azimuthally polarized output mode are shown in Figs. 8(a)–8(e).

In conclusion, we reported the experimental results on an all-fiber WS_2 based passively Q-switching laser to generate CVB. By tuning PCs, both the radially polarized beam and azimuthally polarized beam could be obtained easily. Furthermore, by increasing the pump power, the repetition rate can be tuned from 80 kHz to 120 kHz with minimum duration of 958 ns. Our results not only proved the excellent performance of WS_2 but also provide a simple and efficient method for generating Q-switching CVBs.

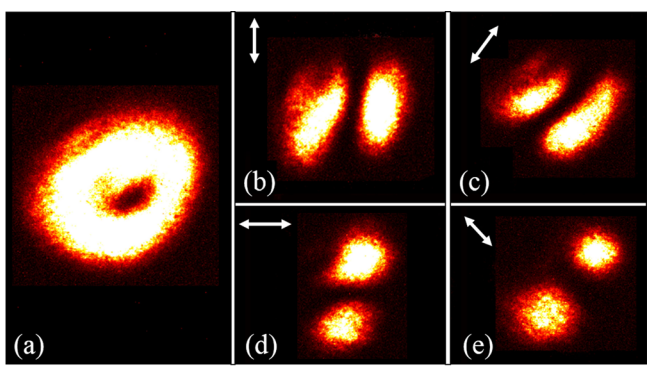

FIG. 8. Intensity distributions of azimuthally polarized laser beam. (a) Azimuthally polarized without a polarizer; (b) and (e) azimuthally polarized after passing through a linear polarizer with transmission axis orientation denoted by arrows.

The authors would thank the support of National Natural Science Foundation of China (Nos. 11374285 and U1330104).

[1]K. S. Novoselov, A. K. Geim1, S. V. Morozov, D. Jiang, M. I. Katsnelson, I. V. Grigorieva1, S. V. Dubonos, and A. A. Firsov, "Two-dimensional gas of massless Dirac fermions in Graphene," Nature **438**, 197–200 (2005).
[2]F. Bonaccorso, Z. P. Sun, T. Hasan, and A. C. Ferrari, "Graphene photonics and optoelectronics," Nat. Photonics **4**, 611–622 (2010).
[3]X. T. Gan, R. J. Shiue, Y. D. Gao, I. Meric, T. F. Heinz, K. Shepard, J. Hone, S. Assefa, and D. Englund, "Chip-integrated ultrafast graphene photodetector with high responsivity," Nat. Photonics **7**, 883–887 (2013).
[4]Q. L. Bao, H. Zhang, Y. Wang, Z. H. Ni, Y. L. Yan, Z. X. Shen, K. P. Loh, and D. Y. Tang, "Atomic-layer graphene as a saturable absorber for ultrafast pulsed lasers," Adv. Funct. Mater. **19**, 3077–3083 (2009).
[5]Z. P. Sun, T. Hasan, F. Torrisi, D. Popa, G. Privitera, F. Q. Wang, F. Bonaccorso, D. M. Basko, and A. C. Ferrari, "Graphene mode-locked ultrafast laser," ACS Nano **4**, 803–810 (2010).
[6]D. Popa, Z. Sun, F. Torrisi, T. Hasan, F. Wang, and A. C. Ferrari, "Sub 200 fs pulse generation from a graphene mode-locked fiber laser," Appl. Phys. Lett. **97**, 203106 (2010).
[7]D. Popa, Z. Sun, T. Hasan, F. Torrisi, F. Wang, and A. C. Ferrari, "Graphene Q-switched, tunable fiber laser," Appl. Phys. Lett. **98**, 073106 (2011).
[8]F. Bernard, H. Zhang, S. Gorza, and P. Emplit, "Towards mode-locked fiber laser using topological insulators," in Advanced Photonics Congress, OSA Technical Digest (Optical Society of America, 2012), Paper No. NTh1A.5.
[9]C. J. Zhao, H. Zhang, X. Qi, Y. Chen, Z. T. Wang, S. C. Wen, and D. Y. Tang, "Ultra-short pulse generation by a topological insulator based saturable absorber," Appl. Phys. Lett. **101**, 211106 (2012).
[10]J. Sotor, G. Sobon, K. Grodecki, and K. M. Abramski, "Mode-locked erbium-doped fiber laser based on evanescent field interaction with Sb_2Te_3 topological insulator," Appl. Phys. Lett. **104**, 251112 (2014).
[11]Y. Chen, C. J. Zhao, H. H. Huang, S. Q. Chen, P. H. Tang, Z. T. Wang, S. B. Lu, H. Zhang, S. C. Wen, and D. Y. Tang, "Self-assembled topological insulator: Bi_2Se_3 membrane as a passive Q-switcher in an erbium-doped fiber laser," J. Lightwave Technol. **31**, 2857 (2013).
[12]S. X. Wang, H. H. Yu, H. J. Zhang, A. Z. Wang, M. W. Zhao, Y. X. Chen, L. M. Mei, and J. Y. Wang, "Broadband few-layer MoS_2 saturable absorbers," Adv. Mater. **26**, 3538–3544 (2014).
[13]M. Zhang, R. C. T. Howe, R. I. Woodward, E. J. R. Kelleher, F. Torrisi, G. H. Hu, S. V. Popov, J. R. Taylor, and T. Hasan, "Solution processed MoS_2-PVA composite for sub-bandgap mode-locking of a wideband tunable ultrafast Er:fiber laser," Nano. Res. **8**, 1522–1534 (2015).
[14]H. Liu, A. P. Luo, F. Z. Wang, R. Tang, M. Liu, Z. C. Luo, W. C. Xu, C. J. Zhao, and H. Zhang, "Femtosecond pulse erbium-doped fiber laser by a few-layer MoS_2 saturable absorber," Opt. Lett. **39**, 4591–4594 (2014).
[15]R. I. Woodward, E. J. R. Kelleher, R. C. T. Howe, G. Hu, F. Torrisi, T. Hasan, S. V. Popov, and J. R. Taylor, "Tunable Q-switched fiber laser based on saturable edge-state absorption in few-layer molybdenum disulfide (MoS_2)," Opt. Express **22**, 31113–31122 (2014).
[16]H. D. Xia, H. P. Li, C. Y. Lan, C. Li, X. X. Zhang, S. J. Zhang, and Y. Liu, "Ultrafast erbium-doped fiber laser mode-locked by a CVD-grown molybdenum disulfide (MoS_2) saturable absorber," Opt. Express **22**, 17341–17348 (2014).
[17]D. Mao, Y. D. Wang, C. J. Ma, L. Han, B. Q. Jiang, X. T. Gan, S. J. Hua, W. D. Zhang, T. Mei, and J. L. Zhao, "WS_2 mode-locked ultrafast fiber laser," Sci. Rep. **5**, 7965 (2015).
[18]C. Janisch, Y. X. Wang, D. Ma, N. Mehta, A. L. Eljas, N. P. López, M. Terrones, V. Crespi, and Z. W. Liu, "Extraordinary second harmonic generation in tungsten disulfide monolayers," Sci. Rep. **4**, 5530 (2014).
[19]X. Zheng, Y. W. Zhang, R. Z. Chen, X. A. Cheng, Z. J. Xu, and T. Jiang, "Z-scan measurement of the nonlinear refractive index of monolayer WS_2," Opt. Express **23**, 15616–15623 (2015).

[20]K. Wu, X. Y. Zhang, J. Wang, X. Li, and J. P. Chen, "WS_2 as a saturable absorber for ultrafast photonic applications of mode-locked and Q-switched lasers," Opt. Express **23**, 11453–11461 (2015).
[21]G. Sobon, J. Sotor, and K. M. Abramski, "All-polarization maintaining femtosecond Er-doped fiber laser mode-locked by graphene saturable absorber," Laser Phys. Lett. **9**, 581–586 (2012).
[22]G. Sobon, J. Sotor, J. Jagiello, R. Kozinski, K. Librant, M. Zdrojek, L. Lipinska, and K. M. Abramski, "Linearly polarized, Q-switched Er-doped fiber laser based on reduced graphene oxide saturable absorber," Appl. Phys. Lett. **101**, 241106 (2012).
[23]Q. W. Zhan, "Cylindrical vector beams: From mathematical concepts to applications," Adv. Opt. Photonics **1**, 1–57 (2009).
[24]D. Pohl, "Operation of a ruby-laser in purely transverse electric mode TE_{01}," Appl. Phys. Lett. **20**, 266 (1972).
[25]Q. W. Zhan and J. R. Leger, "Focus shaping using cylindrical vector beams," Opt. Express **10**, 324–331 (2002).
[26]R. Dorn, S. Quabis, and G. Leuchs, "Sharper focus for a radially polarized light beam," Phys. Rev. Lett. **91**, 233901 (2003).
[27]G. Volpe, G. P. Singh, and D. Petrov, "Optical tweezers with cylindrical vector beams produced by optical fibers," Proc. SPIE **5514**, 283 (2004).
[28]A. Bouhelier, F. Ignatovich, A. Bruyant, C. Huang, G. C. D. Francs, J. C. Weeber, A. Dereux, G. P. Wiederrecht, and L. Novotny, "Surface plasmon interference excited by tightly focused laser beams," Opt. Lett. **32**, 2535–2537 (2007).
[29]L. Novotny, M. R. Beversluis, K. S. Youngworth, and T. G. Brown, "Longitudinal field modes probed by single molecules," Phys. Rev. Lett. **86**, 5251–5254 (2001).
[30]V. G. Niziev and A. V. Nesterov, "Influence of beam polarization on laser cutting efficiency," J. Phys. D: Appl. Phys. **32**, 1455–1461 (1999).
[31]E. A. J. Marcatili, R. A. Schmeltzer, and B. S. Techn, "Hollow metallic and dielectric waveguides for long distance optical transmission and lasers," Bell Syst. Tech. J. **43**, 1783–1809 (1964).
[32]B. Sun, A. T. Wang, L. X. Xu, C. Gu, Z. X. Lin, H. Ming, and Q. W. Zhan, "Low-threshold single-wavelength all-fiber laser generating cylindrical vector beams using a few-mode fiber Bragg grating," Opt. Lett. **37**, 464 (2012).
[33]L. Gong, Y. X. Ren, W. W. Liu, M. Wang, M. C. Zhong, Z. Q. Wang, and Y. M. Li, "Generation of cylindrically polarized vector vortex beams with digital micromirror device," J. Appl. Phys. **116**, 183105 (2014).
[34]D. Lin, K. G. Xia, R. X. Li, X. J. Li, G. Q. Li, K. I. Ueda, and J. L. Li, "Radially polarized and passively Q-switched fiber laser," Opt. Lett. **35**, 3574–3576 (2010).
[35]K. G. Zhou, M. Zhao, M. J. Chang, Q. Wang, X. Z. Wu, Y. L. Song, and H. L. Zhang, "Size-dependent nonlinear optical properties of atomically thin transition metal dichalcogenide nanosheets," Small **11**(6), 694–701 (2015).
[36]J. Lin, Y. Y. Hu, C. J. Chen, L. X. Xu, and C. Gu, "Wavelength-tunable Yb-doped passively Q-switching fiber laser based on WS_2 saturable absorber," Opt. Express **23**, 29059–29064 (2015).
[37]M. W. Jung, J. S. Lee, J. Park, J. H. Koo, Y. M. Jhon, and J. H. Lee, "Mode-locked, 1.94-μm, all-fiberized laser using WS_2-based evanescent field interaction," Opt. Express **23**, 19996–20006 (2015).
[38]D. Yang and R. F. Frindt, "Li-intercalation and exfoliation of WS_2," J. Phys. Chem. Solids **57**, 1113–1116 (1996).
[39]N. Perea-López, A. L. Elías, A. Berkdemir, A. Castro-Beltran, H. R. Gutiérrez, S. M. Feng, R. T. Lv, T. Hayashi, F. López-Urías, S. Ghosh, B. Muchharla, S. K. Talapatra, H. Terrones, and M. Terrones, "Photosensor device based on few-layered WS_2 films," Adv. Funct. Mater. **23**, 5511–5517 (2013).
[40]J. N. Coleman, M. Lotya, A. O'Neill, S. D. Bergin, P. J. King, U. Khan, K. Young, A. Gaucher, S. De, R. J. Smith, I. V. Shvets, S. K. Arora, G. Stanton, H. Y. Kim, K. Lee, G. T. Kim, G. S. Duesberg, T. Hallam, J. J. Boland, J. J. Wang, J. F. Donegan, J. C. Grunlan, G. Moriarty, A. Shmeliov, R. J. Nicholls, J. M. Perkins, E. M. Grieveson, K. Theuwissen, D. W. McComb, P. D. Nellist, and V. Nicolosi, "Two-dimensional nanosheets produced by liquid exfoliation of layered materials," Science **331**, 568–571 (2011).
[41]R. Zheng, C. Gu, A. T. Wang, L. X. Xu, and H. Ming, "An all-fiber laser generating cylindrical vector beam," Opt. Express **18**, 10834–10838 (2010).